JOURNAL OF CATALYSIS 63, 83–93 (1980)

Kinetics and Mechanism of the CO shift on Cu/ZnO

1. Kinetics of the Forward and Reverse CO Shift Reactions

T. VAN HERWIJNEN[1] AND W. A. DE JONG[2]

Laboratory of Chemical Technology, Delft University of Technology, 136 Julianalaan, Delft, The Netherlands

Received May 5, 1978; revised July 13, 1979

The CO shift reaction over a Cu/ZnO catalyst, $CO + H_2O \rightleftarrows CO_2 + H_2$, has been studied to obtain kinetic evidence for the supposition that it proceeds via a formate-type intermediate on the catalyst surface. The results can be described with Langmuir-type kinetic equations and indicate that both the forward and reverse CO shift are characterized by a relatively stable intermediate formed from one molecule of each of the reactants, $CO \cdot H_2O$ and $CO_2 \cdot H_2$, respectively. The decomposition of this complex is rate determining; in both cases the copper surface coverage by the complex is relatively high and varies little in the temperature range of commercial application of the shift reaction.

NOMENCLATURE

Symbols

ξ	conversion
W	catalyst weight
F_{CO}	mole flow of CO
x	composition parameter
x_j	mole fraction of component j
p_j	partial pressure in bar of component j
p	total pressure
k	rate constant
K_j	adsorption equilibrium constant for component j
E	activation energy
E_a	apparent energy of activation
r	initial rate of reaction
m	exponent in rate equation

Indices

f	forward
r	reverse
o	observed
c	calculated

INTRODUCTION

The CO shift conversion,

$$CO + H_2O \rightleftarrows CO_2 + H_2 \qquad (\Delta H_s^\circ = -41.1 \text{ kJ/mole}),$$

is among the oldest catalytic reactions applied industrially to produce hydrogen or ammonia synthesis gas. Most papers on this reaction published to date deal with catalysis by oxides, particularly with iron oxide-based catalysts (*1*). Much less information is available in the literature on the low-temperature Cu/ZnO shift catalyst, which is widely used commercially since about 1960. We have studied the CO shift over this catalyst to obtain information on the kinetics and mechanism. The results may not only be relevant for the water–gas shift conversion but also for methanation for the production of SNG, where the shift conversion takes place as a side reaction (*2*). Results are reported below of a kinetic study over Cu/ZnO catalyst of the forward as well as the reverse shift conversion. Some observations regarding the mechanism are made in a second paper (*3*).

[1] Present address: Shell Coal International Ltd., London, U. K.

[2] To whom correspondence should be addressed.

0021-9517/80/050083-11$02.00/0

The CO shift conversion is often looked upon as an oxygen transfer reaction in which CO is oxidized by water, the catalyst acting as an oxygen transfer agent. Such reactions can be split into two consecutive half-reactions in which catalyst sites, s, are oxidized and reduced:

$$H_2O + s \rightleftarrows sO + H_2$$

and

$$CO + sO \rightleftarrows CO_2 + s.$$

This type of redox system is characterized by two features. Firstly, both reactions must be possible thermodynamically; although an exact calculation of equilibrium constants and heats of reaction is impossible because of the difference between surface thermodynamic properties and bulk properties, the order of magnitude should be correct when the calculations are based on bulk properties. Secondly, the two reactions must proceed independently to a certain extent if a redox mechanism applies. It is well-established that the active form of the iron/chromium oxide catalyst has the composition of magnetite, Fe_3O_4 (*4*). Assuming Fe_3O_4 to be the active ingredient of the catalyst, the CO shift reaction will proceed via the half-reactions:

$$CO + Fe_3O_4 \rightleftarrows CO_2 + 3\ \text{“FeO”}$$

and

$$H_2O + 3\ \text{“FeO”} \rightleftarrows H_2 + Fe_3O_4.$$

In these equations, “FeO” denotes some reduced form of iron oxide. Boreskov *et al.* (*5*) have shown that such half-reactions can indeed proceed independently at about equal rates, which correspond to the rate observed for a mixed CO and water feed.

A similar explanation is improbable in the case of Cu-containing catalysts. Half-reactions can be formulated for the oxidation of Cu to Cu_2O or CuO by water and for the reduction of these oxides by CO. The latter step is known to proceed smoothly at 200°C (*6, 7*), but neither oxide is formed from water and Cu up to 800°C in the absence of oxygen (*8*). Moreover, thermodynamic calculations show that formation of Cu_2O from water and copper is very improbable, the free energy of reaction being about +80 kJ/mole cuprous oxide. Of course, this does not entirely preclude the formation of a superficial oxide layer and chemisorption of water may still occur.

Armstrong and Hilditch (*9*), who were the first to postulate the redox mechanism for iron oxide catalysts, come to the same conclusion. These authors suppose that on Cu/ZnO catalysts formic acid is the intermediate, arguing that the CO shift over copper sets in at about the same temperature as the decomposition of HCOOH. On oxide catalysts formate ions have been detected by infrared spectroscopy during the forward as well as the reverse shift reactions (*10*). A study of formic acid decomposition on copper showed high coverages with surface formate, acid decomposition of which is rate determining (*11*). If the formic acid intermediate hypothesis applies to the CO shift over Cu catalysts, one would expect a rather stable intermediate formed from 1 mole of CO and 1 mole of water.

The aim of the study reported here was to find kinetic evidence for such a formate mechanism of the CO shift. Therefore, the forward and reverse shift reactions were studied as well as the decomposition of formic acid, using a commercial Cu/ZnO catalyst.

Data published in the literature do not provide the information required to identify the rate-determining step of the CO shift over Cu/ZnO. Kinetic models proposed for this reaction are shown in Table 1. Campbell (*12, 13*) published a kinetic model which “was derived after careful consideration of plant data and semi-technical results,” but the data on which the dimensionless rate equation is based are not reported. The author concludes that with his catalyst the CO shift is strongly pore diffu-

TABLE 1

Published Kinetic Models for the Water–Gas Reaction on LTS Catalysts

Campbell (*13*)	$r = \dfrac{k \cdot p_{CO} \cdot p_{H_2O}}{(1 + K_1 p_{CO} + K_2 p_{H_2O} + K_3 p_{CO_2} + K_4 p_{H_2})^2}(1 - \beta)$
Moe (*14*)	$r = k \cdot p_{CO} \cdot p_{H_2O}(1 - \beta)$
Shchibrya (*15*)	$r = k \cdot p_{H_2O} \cdot \dfrac{p_{CO}}{A \cdot p_{H_2O} + p_{CO_2}} \cdot (1 - \beta)$
Kul'kova–Temkin (*17*)	$r = k \cdot p_{CO} \cdot \left(\dfrac{p_{H_2O}}{p_{H_2}}\right)^{0.5}(1 - \beta)$
Goodridge–Quazi (*18*)	$r = k \cdot p_{CO}{}^a \cdot p_{H_2O}{}^b \cdot p_{CO_2}{}^c \cdot p_{H_2}{}^d$
	$\beta = \dfrac{p_{CO_2} \cdot p_{H_2}}{p_{CO} \cdot p_{H_2O}} \cdot \dfrac{1}{K_{eq}}$

sion limited above 200°C. The chief value of Campbell's rate equation clearly lies in its suitability for reactor design purposes. A similar conclusion is valid for the equation published by Moe (*14*).

Shchibrya *et al.* (*15*) apply their kinetic equation for the iron oxide/chromium oxide-catalyzed shift reaction to measurements on $Cu/ZnO/Cr_2O_3$. This equation was derived assuming an oxidation/reduction mechanism in which the reduction of the catalyst surface by CO is rate determining. However, if a redox mechanism applies to Cu/ZnO, oxidation of the catalyst by water is most likely the rate-determining step. Similar objections apply to the rate equations found by Uchida *et al.* (*16*), who use the Kul'kova–Temkin relation (*17*) which is based on the same assumptions as Shchibrya's equation.

Finally, a power rate equation was published by Goodrich and Quazi (*18*) for a $Cu/ZnO/Cr_2O_3$ catalyst; the authors observed a very low apparent energy of activation, suggestive of diffusional limitations.

The two published studies on the reverse shift reaction (*19, 20*),

$$CO_2 + H_2 \rightleftarrows CO + H_2O,$$

do not provide a sufficient basis in the context of the present work. Rates of formic acid decomposition are not reported for any of the catalysts mentioned in the literature.

EXPERIMENTAL

Equipment. The continuous flow equipment of Fig. 1 was used in the kinetic study of the reaction of CO with water. The system allows addition of the reaction products, CO_2 and H_2, to examine their effects on the rate. The feed gases were fed from bottles, dried over molecular sieves (3A), and metered with precision flow controllers (1). The flow rates were obtained from the pressure drop across stainless steel capillaries immersed in a thermostatic bath. After mixing the combined feed gases were freed of oxygen in reactor (2) filled with Cu/SiO_2, BASF R3-11. Distilled and degassed water was fed by pump (3), the flow rate being calculated from readings of a microburette obtained after closing the valve between the pump and the water storage vessel. The water was evaporated in evaporator (4) and mixed with the other gases. Condensation was avoided by heating the stainless steel lines leading to the reactor section. The 2-ml stainless steel reactor was immersed in a fluidized bed thermostat (5) containing glass beads with an average diameter of 0.1 mm. The temperature could be controlled to within 1°C. The temperature in the reactor was measured with a Chromel–Alumel thermocouple placed in the center of the reactor, its emf being determined with a compensator. After completion of the measurements,

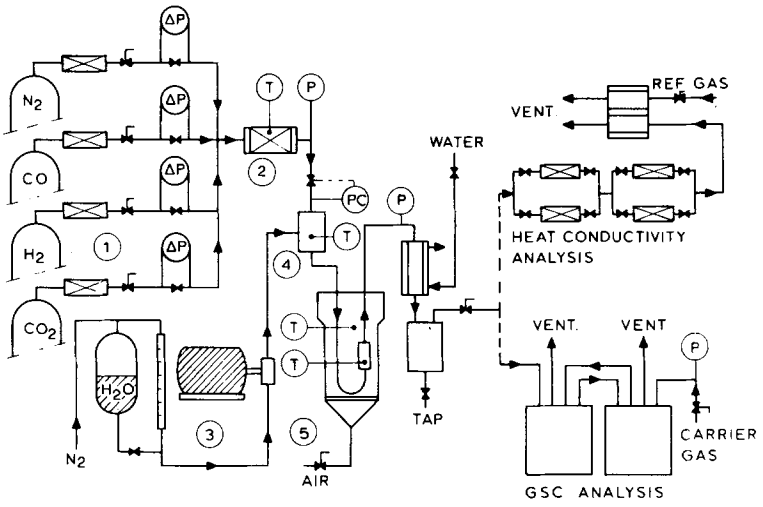

FIG. 1. Flow apparatus employed for experiments on the forward CO conversion.

thermocouple plus compensator were calibrated against a precision resistance thermometer. The reactor was charged with 0.5- to 2.0-g crushed catalyst, particle size 0.35–0.42 mm. This size is sufficiently small to ensure a good approach to plug flow.

Analysis. In most kinetic experiments gas/solid chromatography was used to analyze the product gases after removal of the water. A molecular sieve (5A) column was employed, with He or H_2 as the carrier gas. The feed contained CO as well as N_2 in an accurately known ratio; the CO conversion could be calculated from the ratios of the peak areas of nitrogen and carbon monoxide before and after the reaction. In a few experiments, mostly when working at pressures above 1 bar, the composition of the product gas was monitored by continuously recording the difference in heat conductivity between a reference gas and the product gas from which water and carbon dioxide had been removed completely.

The gas chromatographic method (gc) is somewhat more reliable than the conductivity analysis. Firstly, gc allows the use of N_2 as an internal standard and, secondly, extreme drying and CO_2 removal are not necessary. Moreover, the determination of the heat conductivity difference with thermistors is sensitive toward disturbances like a baseline shift and small temperature variations of the diffusion katharometer used. However, if used with care, the heat conductivity method is more accurate at low conversions, i.e., from 1 to 5%, since even small conversions result in a sharp increase in conductivity because of the hydrogen produced.

The equipment in which the reverse shift reaction was studied was similar, except for the simpler feed system: water dosage is not required here. Analyses were invariably made by gas/solid chromatography.

Materials. The gases were the purest grades available; moisture and oxygen were removed as indicated before. Distilled and degassed water was used. The catalyst was Girdler/Südchemie G 66B. Its main components (unreduced) were CuO (32.2 wt%), ZnO (61.8 wt%), and Fe_2O_3, (1.6 wt%), and the BET surface area before reduction amounted to 22.3 m^2/g (N_2 adsorption). Assuming cylindrical pores, the average pore diameter was about 12.5 nm. Pores smaller than 5 nm were not found.

Procedure. The catalyst was activated by heating to 200°C in a nitrogen flow at a rate of 80°C/h. Reduction was accomplished in 4–10 h using an activation gas consisting of 1–5% H_2 in nitrogen. Such careful activation is necessary: if, for instance, high

partial pressures of H_2 or high temperatures are applied the catalyst may show an activity below the optimum because some small amount of ZnO may be reduced along with the CuO, giving rise to the formation of α-brass. Further information on this subject is given in a previous paper (*21*).

After catalyst reduction was complete, a gas mixture consisting of CO, water, and nitrogen was fed to the reactor. Initially, the catalyst activity declines but the deactivation slows down to an acceptable rate after a few days of continuous operation. In determining the kinetics, the temperatures were varied in a random manner, and a check on catalyst activity was carried out after each series at a given temperature. It was not necessary to correct for loss of catalyst activity.

The rate of reaction was calculated from

$$r = \frac{\xi}{(W/F_{CO})}. \qquad (1)$$

This rate is equal to the initial rate as long as the conversion is kept low since initially a linear relation exists between conversion, ξ, and reciprocal space velocity, W/F_{CO}. The experiments were designed to give conversions below 12% of equilibrium so that for the reactions examined here the error caused by the assumption of linearity, i.e., the difference between calculated rate and true rate, is generally less than 5% relative (*22*).

RESULTS

Forward shift reaction. Initial rates of the forward CO shift reaction measured between 172 and 228°C and at atmospheric pressure are shown in Fig. 2 as a function of x, the mole fraction of water in the feed. Nitrogen was added in a fixed molar ratio of 1.13 moles N_2/mole CO as an inert internal standard. The feed gas composition can be described with one single parameter, x:

$$x_{H_2O} = p_{H_2O} = x,$$
$$x_{CO} = p_{CO} = 0.47\,(1 - x),$$
$$x_{N_2} = p_{N_2} = 0.53\,(1 - x).$$

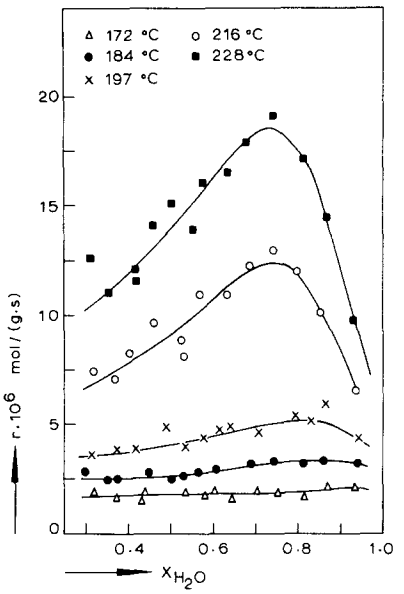

FIG. 2. Initial rate of reaction of the forward CO conversion. Feed molar ratio $CO/N_2 = 0.89$.

The indicated temperatures are the averages for each series; individual temperatures have been used in correlating the data.

Qualitatively, the following conclusions can be drawn from Fig. 2:

(i) at the lower temperatures, the observed rate depends weakly on feed composition;

(ii) at higher temperatures, the maximum shifts somewhat to the left and becomes more pronounced.

These conclusions point to a substantial surface coverage at low temperatures. Moreover, the behavior at higher temperatures, where surface coverage decreases, suggests a description by a parabolic rate equation containing a term

$$r \cong kx(1 - x) \cong kx_{H_2O}x_{CO}. \qquad (2)$$

As a next step, the observed data were converted into a rate equation assuming Langmuir adsorption. Although the underlying assumptions have frequently been criticized as being oversimplifications, they often lead to useful kinetic models describing the kinetics within experimental accu-

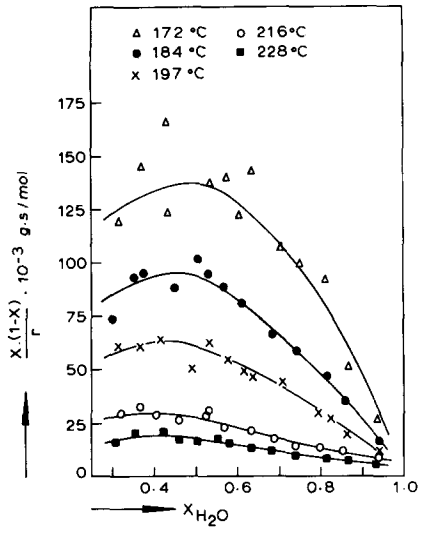

FIG. 3. Plot of (DENOMINATOR)^m versus x for the forward shift reaction.

racy. Moreover, Langmuir-type rate equations are often qualitatively consistent with other independent observations and may allow physical interpretation. Depending on the rate-determining step, different rate equations can be formulated of the general form

$$r = \frac{k(\text{GRADIENT})}{(\text{DENOMINATOR})^m} = \frac{k \cdot x(1-x)}{(\text{DENOMINATOR})^m}. \quad (3)$$

An equilibrium term need not be added because reaction products CO_2 and H_2 are absent.

The form of (DENOMINATOR)^m, a function of composition and temperature, was established from plots of $x(1-x)/r$ against x. These plots (Fig. 3) show maxima close to 0.5, which implies that DENOMINATOR is quadratic in itself, containing a term like $x(1-x) \cong x_{H_2O} \cdot x_{CO}$, and that m is equal to 1. However, DENOMINATOR must be more complex because the plots of rate against composition (Fig. 2) are asymmetric, showing maxima close to 0.3. This can be accounted for by adding another term proportional to p_{CO}. Thus we have:

$$\text{DENOMINATOR} = 1 + k_1 x(1-x) + k_2(1-x).$$

A water adsorption term may still be present; thus, the most general rate equation becomes:

$$r = \frac{kx_{H_2O}x_{CO}}{1 + K_{CO\cdot H_2O}x_{CO}x_{H_2O} + K_{CO}x_{CO} + K_{H_2O}x_{H_2O}} = \frac{kx(1-x)}{1 + K_1x(1-x) + K_2(1-x) + K_3x}. \quad (4)$$

This rate equation was fitted to the measured data, each of the adsorption constants being allowed to be zero (Z), finite but independent of the temperature (C), or dependent on T via an Arrhenius-type function (T). The latter was also assumed for the rate constant, k. A nonlinear regression routine was applied to the resulting 27 rate equations, the objective being to minimize the sum of squares of the *relative* deviations between observed rate, $r_{o,i}$, and the corresponding calculated rates, $r_{c,i}$:

$$\text{minimize: } Q = \sum_{i=1}^{n} \left(\frac{r_{o,i} - r_{c,i}}{r_{o,i}} \right)^2. \quad (5)$$

The variances about regression computed from Q_{min} were subjected to the F test to assess the significance of the differences between the variances of the models. Although the F test strictly applies to linear models only, it can be used as an approximation for discrimination between nonlinear models. Figure 4 shows the variances in what may be called a "model space." The variances in the shaded areas are not significantly different at the 95% probability level from the lowest variance value, 0.0178. It follows that models in which the term

$$K_{CO\cdot H_2O} \cdot x_{H_2O} \cdot x_{CO}$$

is absent do not represent the data as well

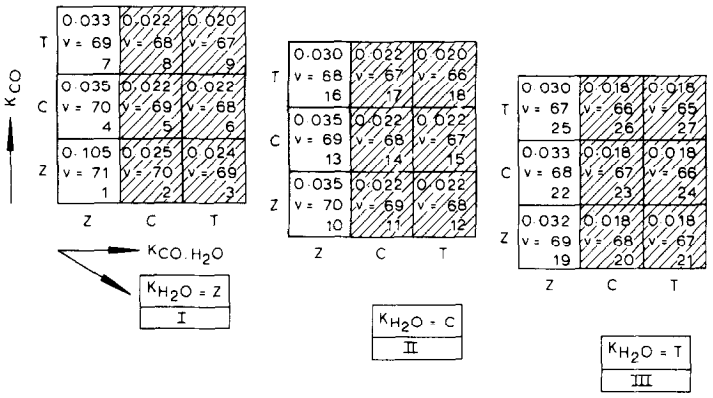

FIG. 4. Variance about regression for the different models in "model space." ν is the number of degrees of freedom of the variance.

as do the other models. Models in which K_2 and K_3 are present as constants give mathematically dependent models. Thus, models 5, 11, and 14 and models 6, 12, and 15 are groups of mathematically identical models and discrimination within these groups on the basis of the data presented here is not possible. The number of model equations is further reduced by considering that addition of an adsorption term for water results at most in a slight but statistically insignificant decrease of the variance. Thus, six models of the first square in Fig. 4 are left.

Apparent activation energies and surface coverages were calculated for four of the six remaining models using

$$\theta_j = \frac{K_j P_j}{\text{DENOMINATOR}} \qquad (6)$$

and

$$E_a = \frac{\partial \ln r}{\partial\, 1/RT}. \qquad (7)$$

The results indicate:

—high coverages by the mixed complex and CO, both of which vary relatively little with the temperature over the range examined (Fig. 5);

—little variation of the apparent activation energy, which is constant at 16.0 kcal/mole for model 5 and varies between 15.4 and 16.4 for model 6 and from 15.5 to 16.5 for model 8.

The above observations show that it is sufficient to include temperature-independent adsorption terms for CO · H_2O as well as CO in the final model while observing, however, that this is a mathematical rather than a physical representation of the measured reaction rates. As the kinetics will be discussed below in terms of reaction rates

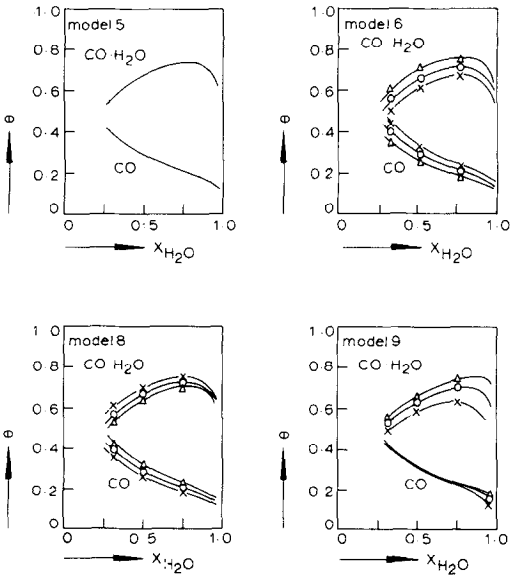

FIG. 5. Surface composition as calculated from models 5, 6, 8, and 9 for the forward reaction. Δ = 175°C, O = 200°C, X = 225°C.

rather than model parameter values, this approach serves the present purpose.

Thus, model 5 was selected to represent the data on the initial rate of the forward shift reaction:

$$r_f = \frac{25.8 \times 10^3 \exp(-16{,}000/RT) \cdot p_{CO} p_{H_2O}}{1 + 127 p_{CO} p_{H_2O} + 26 p_{CO}} \text{ moles/(g} \cdot \text{s)}. \quad (8)$$

Reverse shift reaction. The measurements and the kinetic modeling on the reverse shift reaction

$$CO_2 + H_2 \rightleftarrows CO + H_2O$$

proceeded along the same lines as those of the forward CO shift. There were, however, some differences:

(i) Nitrogen was not added to the reactor feed; conversions have been calculated from the product (CO) concentration in the reactor effluent.

(ii) Large product samples had to be taken because the equilibrium conversion in the temperature range examined, 195–225°C, is approximately 3%. With the available equipment, conversions of about 0.05% could be measured with the required accuracy.

(iii) Catalyst activity decline was observed (Fig. 6); the activities were normalized to the activity level at 700 h. This reduces observed differences in the rates of reaction measured at different catalyst life (Fig. 7) to an acceptable degree.

The initial rate data obtained are shown in Fig. 8 in the form of a plot of the rate against the mole fraction of CO_2 in the feed. The same observations as those made with regard to the corresponding data for the forward shift reaction apply. The selected rate equation has the following form:

$$\frac{k \cdot x_{CO_2} \cdot (1 - x_{CO_2})}{1 + K \cdot x_{CO_2}(1 - x_{CO_2}) + B \cdot x_{CO_2}}. \quad (9)$$

The term $B \cdot x_{CO_2}$ is positive if it originates from CO_2 adsorption and negative in the case of hydrogen adsorption because it should then read: $B'(1 - x_{CO_2})$. Upon differentiation of r to x_{CO_2} and considering that the maximum rate occurs at $x_{CO_2} > 0.5$, one finds that B is a negative constant, which means that the added term in the denominator represents adsorption of hydrogen. This does not imply that CO_2 is not adsorbed, but merely that the coverage by H_2 is larger than that by CO_2. It was preferred to incorporate only $K \cdot x_{H_2}$ in the denominator because otherwise the number of parameters increases without due compensation in the form of a smaller variance.

Following the procedure outlined earlier, the variances for models of the general form

$$r_r = \frac{k \cdot p_{CO_2} p_{H_2}}{1 + K_{CO_2 \cdot H_2} p_{CO_2} p_{H_2} + K_{H_2} \cdot p_{H_2}} \quad (10)$$

were computed. The results (Fig. 9) indi-

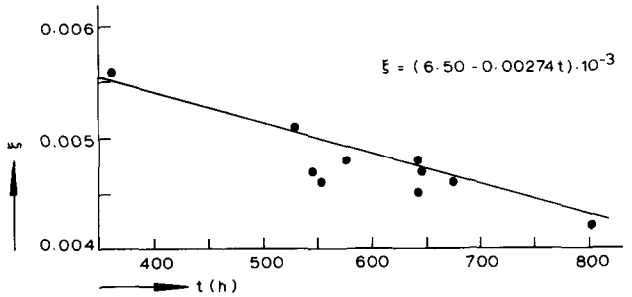

FIG. 6. Conversion at reference condition as a function of time. $x_{CO_2} = 0.5$, $x_{H_2} = 0.5$, $T = 240$°C.

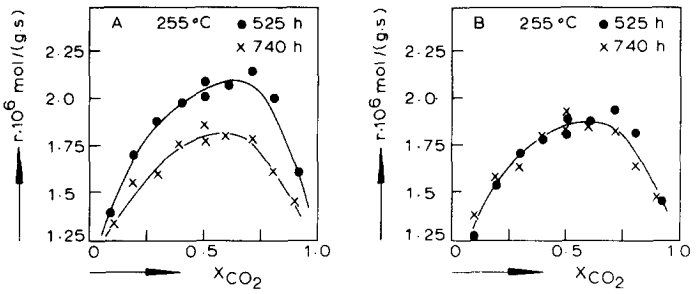

FIG. 7. Correction for catalyst deactivation. (A) Uncorrected, (B) corrected.

cate that both adsorption constants must be nonzero. The parameters of the models in the preferred area of the model plane were used to calculate E_a, Θ_{H_2}, and $\Theta_{CO_2 \cdot H_2}$ for variable ranges explored in the experiments (see Fig. 10). High coverages by the complex $CO_2 \cdot H_2$ are found. The apparent activation energy for the four models, 5, 6, 8, and 9, are all between 23 and 29 kcal/mole, the average being 25.0 kcal/mole. Calculations in which the exponent in the denominator, m, was allowed to vary did not give a significantly improved fit and the calculated values of m were close to unity. On the basis of the above, the initial rate model 6 was selected to represent the experimental data:

$$r_r = \frac{4.29 \times 10^5 \exp(-23{,}500/RT) \cdot p_{CO_2} \cdot p_{H_2}}{1 + 40 p_{CO_2} p_{H_2} + 3.66 \times 10^{-6} \exp(13{,}100/RT) p_{H_2}} \text{ moles/(g} \cdot \text{s)}. \quad (11)$$

DISCUSSION

The presence of an intermediate surface complex, $CO \cdot H_2O$, is revealed beyond doubt by the results of the kinetic study on the shift reaction. The coverage by this complex is rather high, viz., about 75%. The rate equation for the forward shift can either be regarded as describing a reaction between adsorbed CO and water vapor,

$$r_f = \frac{k}{K_{CO}} \cdot p_{H_2O} \cdot \Theta_{CO},$$

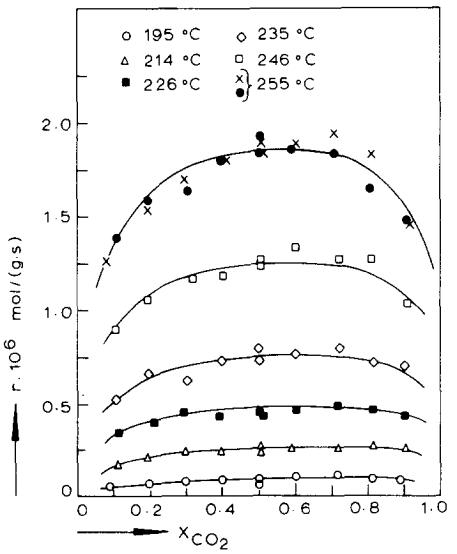

FIG. 8. Rate of the reverse CO shift reaction.

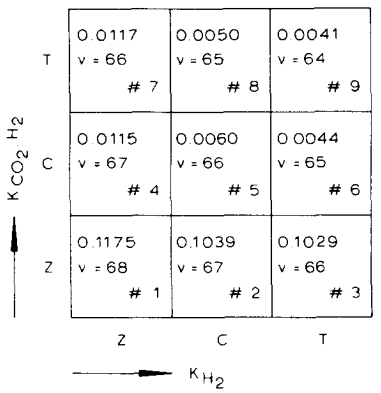

FIG. 9. Variances for the reaction rate models for the reverse shift reaction. Z = Zero, C = constant, T = temperature dependent.

or as referring to the decomposition of an adsorbed complex, $CO \cdot H_2O$,

$$r_f = \frac{k}{K_{CO \cdot H_2O}} \cdot \Theta_{CO \cdot H_2O}.$$

The large coverage found for a complex $CO \cdot H_2O$ makes the second explanation more likely. A further possibility to discriminate between the two rate-determining steps is to carry out experiments at varying pressures. If reaction between adsorbed CO and water vapor is rate determining, an increase of the pressure should give higher rates. When, on the other hand, a surface reaction is controlling, a varying dependence should be expected. At low pressures, where surface coverage is small, the rate should go up linearly with the pressure, or almost so; at high coverages, the rate should be nearly independent of the system pressure.

Experiments up to 6 bar clearly showed that the initial rate of the forward shift does not depend on the pressure (Fig. 11). This points to high surface coverage and rate control by decomposition of the intermediate complex, $CO \cdot H_2O$, or by desorption

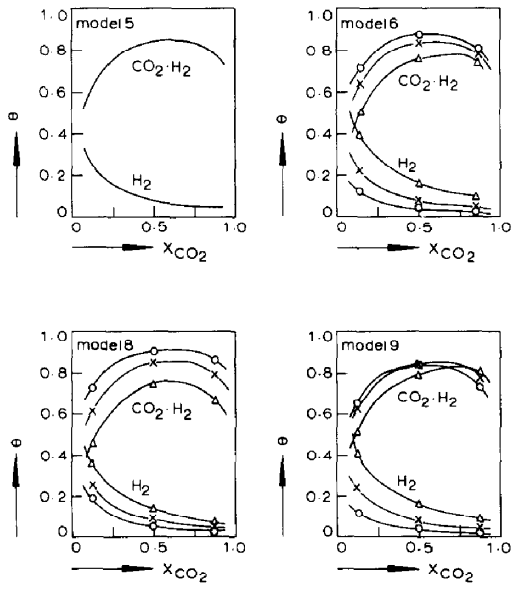

FIG. 10. Surface composition as calculated from models 5, 6, 8, and 9 for the reverse reaction. Δ = 200°C, X = 230°C, 0 = 260°C.

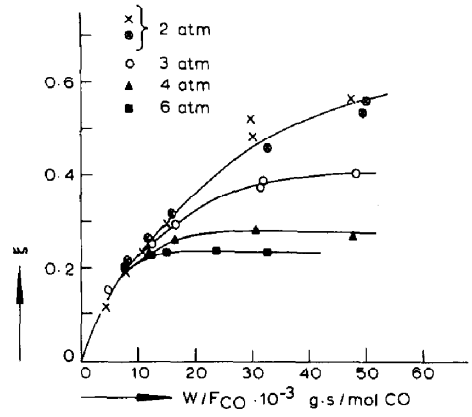

FIG. 11. Conversion at 230°C at varying space velocity and pressure. Feed composition: $x_{CO} = 0.21$, $x_{N_2} = 0.21$, $x_{H_2O} = 0.58$.

rates. Full data on experiments at higher pressure are reported elsewhere (*22*).[3] For the reverse reaction, it can be concluded similarly that the decomposition of the complex $CO_2 \cdot H_2$ is rate determining. It should be noted that the coverages of the surfaces are modeled "implicitly": different model equations made to fit one set of initial rate data show very consistent results for surface coverages and apparent energy of activation, as calculated from Eq. (6) and (7), respectivley. This result is obtained regardless of the quite different model parameter values, which for some models indeed are physically unrealistic. For our present purpose it is, for example, immaterial whether a temperature-dependent or -independent adsorption constant is used in the equation for the rate of the forward shift reaction. Since in both cases it is concluded that the decomposition of the intermediate complex determines the rate, values found for rate constants and corresponding surface coverages depend rather weakly on the rate equation selected. Returning to the original objective of the present work viz., to establish whether the CO shift proceeds via a similar surface intermediate as the decomposition of for-

[3] The results obtained at higher pressures are also discussed in our second paper on the CO shift (*3*).

mic acid, it can be said now that the forward and reverse CO shifts are characterized by a surface complex having the same stoichiometry as formic acid. In other words:

$$CO + H_2O \underset{a}{\overset{b}{\rightleftarrows}} (H_2CO_2) \underset{c}{\overset{d}{\rightleftarrows}} CO_2 + H_2.$$

The rate equations indicate that at 220°C the reverse shift reaction is about 40 times slower than the forward shift. Since in both cases the rate of complex formation is higher than the rate of its decomposition, it follows that the rate of step d is 40 times that of step a. If intermediate (H_2CO_2) is the same as the intermediate occurring in the decomposition of formic acid, i.e., a formate, one should find high selectivities toward CO_2 and H_2 in this decomposition. This point will be taken up in the subsequent paper.

The occurrence of a mixed adsorption term in rate Eqs. (6) and (11) has not been recognized before and the rate models proposed here differ significantly from previously published equations. Only the apparent energy of activation calculated from the data of Cherednik *et al.* (*23*) for the Shchibrya equation (*15*) is in agreement with our observations.

ACKNOWLEDGMENTS

We are indebted to many colleagues and in particular to Messrs. P. G. Tjallema, C. W. A. Schram, and P. W. H. Tjan for their contributions to this study. The assistance of Mr. H. van Meerendonk in the nonlinear regression analyses is appreciated.

REFERENCES

1. Wagner, C., *in* "Advances in Catalysis and Related Subjects" (D. D. Eley, H. Pines, and P. B. Weisz, Eds.), Vol. 21, p. 336. Academic Press, New York, 1970.
2. Saletove, D. A., and Thompson, W. J., *Ind. Eng. Chem. Proc. Res. Develop.* **16,** 70 (1977).
3. van, Herwijnen, T., Guczalski, R. T., and de Jong, W. A., *J. Catal.* **63,** 94 (1980).
4. Mars, P., Gorgels, M. J., and Zwietering, P., *in* "Actes du Deuxième Congrès International de Catalyse," p. 2429. Edition Technip, Pars, 1961.
5. Boreskov, G. K., Yur'eva, T. M., and Sergeeva, A. S., *Kinet. Catal. USSR* **11,** 1230 (1970).
6. Garner, W. E., Gray, T. J., and Stone, F. S., *Proc. Roy. Soc. Ser. A* **197,** 294 (1949).
7. Mars, P., *Z. Phys. Chem. Frankfurt am Main* **22,** 309 (1959).
8. Domance, L., *Bull. Soc. Chim. R.* 5, **12,** 111 (1945).
9. Armstrong, E. F., and Hilditch, T. P., *Proc. Roy. Soc. Ser. A* **97,** 265 (1920).
10. Scholten, J. J. F., Mars, P., Menon, P. G., and van Hardeveld, R., "Proceedings, 3rd Int. Congress on Catalysis," p. 881. North-Holland, Amsterdam, 1965.
11. Sachtler, W. M., H., and Fahrenfort, J., *in* "Actes du Deuxième Congrès International de Catalyse," p. 831. Edition Technip, Paris, 1961.
12. Campbell, J. S., *Ind. Eng. Chem. Proc Res. Develop.* **9,** 588 (1970).
13. Campbell, J. S., Craven, P., and Young, P. W., "Catalyst Handbook," p. 109. Wolfe Scientific Books, London, 1970.
14. Moe, J. M., *Chem. Eng. Progr.* **58,** 33 (1962).
15. Shchibrya, G. G., Morozov, N. M., and Temkin, M. I., *Kinet. Catal. USSR* **6,** 1010 (1965).
16. Uchida, H., Isogai, N., Oba, M., and Hasegawa, T., *Bull Chem. Soc. Jap* **41,** 479 (1968).
17. Kul'kova, N. V., and Temkin, M. I., *Zh. Fiz. Kim.* **23,** 695 (1949).
18. Goodridge, F., and Quazi, H. A., *Trans. Inst. Chem. Eng.* **45,** T274 (1967).
19. Barkley, L. W., Corrigan, T. E., Wainwright, H. W., and Sands, A. E., *Ind. Eng. Chem.* **44,** 1066 (1952).
20. Kodama, S., Mazume, A., Fukuba, K., and Fukui, K., *Bull. Chem. Soc. Japan* **28.** 318 (1955).
21. van, Herwijnen, T., and de Jong, W. A., *J. Catal.* **34,** 209 (1974).
22. van, Herwijnen, T., On the Kinetics and Mechanism of the CO shift conversion on a Copper/zinc oxide Catalyst. Thesis, Appendix F. Delft, University of Technology, 1973.
23. Cherednik, E. M., Morozov, N. M., and Temkin, M. I., *Kinet. Catal. USSR* **10,** 494 (1969).